RSC Advances

ROYAL SOCIETY OF CHEMISTRY

www.rsc.org/advances

RSC Advances

COMMUNICATION

Electroless plating of copper nanoparticles on PET fiber for non-enzymatic electrochemical detection of H_2O_2

Received 00th January 20xx,
Accepted 00th January 20xx

DOI: 10.1039/x0xx00000x

www.rsc.org/

Eunju Kim, Narayanasamy Sabari Arul,* Liu Yang and Jeong In Han*

We have fabricated copper nanoparticles (Cu NPs) on polyethylene terephthalate (PET) fiber by electroless plating for the electrochemical detection of hydrogen peroxide (H_2O_2). The structural analysis confirms the formation of Cu NPs on PET fiber and they exhibit a good electrochemical sensing towards H_2O_2 with an excellent sensitivity of 0.387 mA μM^{-1} cm^{-2} with a low detection limit of 2 µM.

1. Introduction

Hydrogen peroxide (H_2O_2) is utilized as a main oxidant in chemical, food and pharmaceutical industries, which have been analyzed by various analytical techniques.[1-5] Among these techniques, the electrochemistry technique has attracted a considerable interest due to its advantages such as a low detection limit, high selectivity and sensitivity can be easily attained.[6]

Nowadays many efforts have been focused to determine non-enzymatic electrochemical sensing of H_2O_2.[6-10] Particularly, copper nanoparticles (Cu NPs) based electrodes have been reported for the detection of glucose and H_2O_2.[11-16] Cu NPs have been widely used as a good electrode materials for the electrochemical platforms due to its high conductivity, ease of preparation, cost effective and good biocompatibility.[17] Ensafi et al., has reported the fabrication and characterization of Cu NPs immobilized on a hybrid chitosan derivative-carbon support for a novel detection of glucose and H_2O_2.[18] Xi et al., has recently reported about the electrodeposition of copper nanoparticles on the poly-*p*-aminobenzene sulfonic acid (poly-ABSA) electropolymerized on glassy carbon electrode (GCE) and studied its electrochemical sensing behaviour towards H_2O_2.[19] Besides, synthesis of carbon nanotubes based fiber and networks have been attracted the interest of researchers toward various potential applications.[20-22] To best of our knowledge, the investigations on non-enzymatic electrochemical detection of H_2O_2 utilizing electroless plating[23,24] of Cu NPs on Polyethylene terephthalate (PET) fiber substrate has not been clarified. In this study we have chosen PET fiber as substrate due to its outstanding mechanical, thermal and dielectric properties and they have been extensively used in microelectronics, membranes and optics.[24]

Department of Chemical and Biochemical Engineering, Dongguk University–Seoul, 100715, South Korea. E-mail: artsabari@gmail.com hanji@dongguk.edu Phone: +82 2 2290 1646, +82 2 2260 3364 Fax: 82-2-2268-8729.

† Electronic Supplementary Information (ESI) available: [XRD spectrum, I-V characteristics curves of conductive PET fiber with Cu NPs were given in ESI]. See DOI: 10.1039/x0xx00000x

Herein, the study reports the data for electroless plating of Cu NPs on polyethylene terephthalate (PET) fiber and investigated their electrochemical sensing performance towards H_2O_2.

2. Experimental details

2.1 Fabrication of conductive Cu NPs on PET fiber

All the chemical reagents used in our experiments were purchased from Sigma Aldrich Ltd and used without any further purification. The fabrication process of electroless plating of Cu NPs on PET fiber substrates require pretreatment including pre-cleaning, sensitization, activating procedures. In a typical synthesis, PET fibers with length of 5 cm were initially pre-cleaned with methanol and acetone for 5 minutes to remove the impurities in the PET fiber substrate. Subsequently, these cleaned PET fibers were transferred into 10 g/L of aqueous solution containing tin (II) chloride dihydrate and 10 mL/L of hydrochloric acid for sensitization, sonicated for 10 min. The activating process was carried out in the solution containing 10 g/L silver (II) nitrate ($AgNO_3$) and 20 µl/L of ammonium hydroxide (NH_4OH) solution, accompanied by sonication for 20 min, and collected the substrate for successive electroless copper plating. Then, 3.25 g/L $CuSO_4.5H_2O$, 40 g/L $NaKC_4H_4O_6.4H_2O$ and 10 g/L NaOH was dissolved in 9.9 ml distilled water and agitated for 10 minutes to obtain a clear solution. Finally, 50 µl of HCHO and 60 µl of CH_3OH were added to the above solution and again agitated till the solution becomes homogenous. The electroless deposition of Cu NPs on PET fiber was carried out for 10 min at three different temperatures, such as 50° C, 60° and 70° C. After electroless plating, the products were rinsed, dried and collected for further characterizations.

2.2 Characterization techniques

The surface morphologies and elemental analysis of Cu NPs on PET fiber were observed by field emission scanning electron microscope and energy dispersive spectroscopy (FESEM, model S-4300, Hitachi, Japan) with an accelerating voltage of 0.8 kV. The EDS (Energy Dispersive X-ray Spectroscopy) was performed on a Horiba (Horiba 7593-H). Atomic Force Microscopy (AFM) imaging was performed on a N8 NEOS (Bruker N8 NEOS, Germany) operating in an non-contact mode with a scan rate of 0.3 lines/sec. The crystal structure of the Cu NPs coated on PET fiber was determined by Rigaku Ultima IV diffractometer using CuKα radiation (λ=0.15406 nm, 40 KV, 40

mA) at a scanning rate of 4 °/min between 20° and 80° (2θ). The Current-Voltage (I-V) measurements of samples were investigated using a Keithley-6517 source meter. The electrochemical measurement was performed using PCE200 Gamry framework electrochemical workstation using a three electrode system in 0.1 M NaOH as the electrolyte. Cu on PET fiber as working electrode, a platinum wire as conter, and Hg/HgO as reference electrode were utilized.

3. Results and Discussion

The surface morphology of electroless plating of Cu NPs on PET fiber was investigated by FESEM analysis. Figure 1 shows the FESEM images of bare PET fiber and Cu NPs coated PET fibers with respect to various reaction temperatures. The SEM images of the bare PET fiber in different magnifications are shown in Fig. 1(a-c).

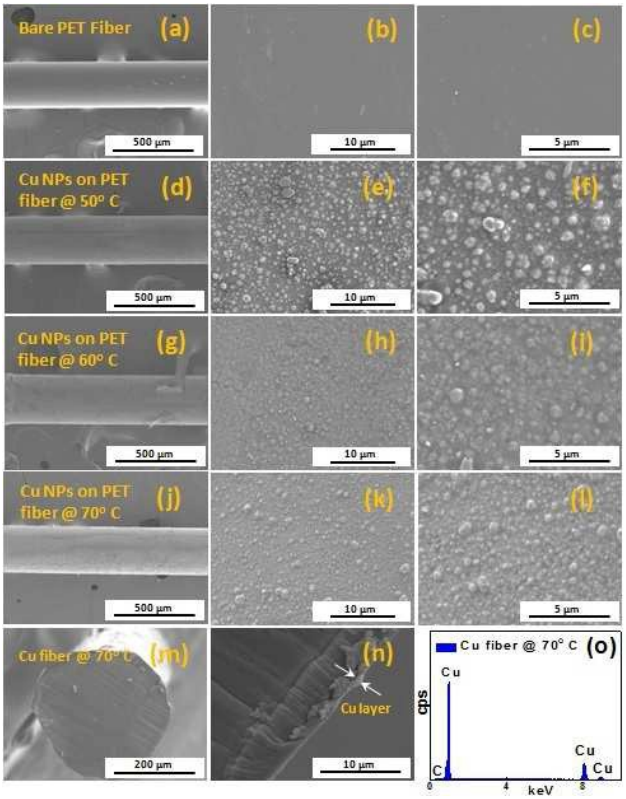

Fig 1. FESEM images of (a-c) displays bare PET fiber; Cu-coated fiber after reaction temperatures (d-f) 50° C (g-i) 60° C and (j-l) 70° C with different magnification; (m, n) Cross sectional FESEM images and (o) EDAX spectrum of 70° C copper-coated fiber.

The FESEM images in Fig. 1 display the morphology of Cu NPs on PET fiber at various reaction temperatures of 50°C (Fig. 1(d-f)), 60° C (Fig. 1(g-i)) and 70° C (Fig. 1(j-l)). It is evident that after electroless plating of Cu, the surface of the PET fibers was coated with large number of Cu NPs whose size ranges about 500 nm, as shown in Fig. 1(d-l). For the reaction temperature of 50° C, Cu NPs coated on PET fiber shows more agglomeration and particle have non-uniform distribution on the surface of PET fiber (Fig. 1(d-f)). As the electroless plating temperature is increased to 60° C, the particle tends to growth further and still the non-uniformity in the size of the Cu particles exist, as shown in Fig. 1(g-i). It is also observed that, the size of Cu particles decreases with increase in reaction temperature from 60° C to 70° C. The Cu NPs deposited on PET fiber at 70° C, as shown in Fig. 1(j-l) exhibit almost uniform distribution when compared to other reaction temperatures, which would be favourable for the electrochemical sensing performance towards H_2O_2. Furthermore, we have carried out the cross sectional view of Cu NPs on PET fiber deposited at 70°C, whose thickness if found to be ~500 nm, as shown in Fig. 1(m & n). The Energy dispersive X-ray spectroscopy (EDX) analysis of conductive Cu fibers is shown in Fig. 1(o). EDX analysis confirms the presence of Cu in the fabricated fiber sample. The spectrum shows a prominent Cu peak in the fabricated PET fiber and no other impurities are observed in the copper coating layer on PET fiber.

In addition to FESEM analysis, Atomic force microscopy (AFM) (Fig. 2) was investigated to characterize the surface morphologies of the Cu NPs on PET fiber prepared at 70°C. Fig. 2 (a-c) displays the two dimensional (2D) AFM images of Cu NPs on PET fiber at 70° C. Fig. 2(b) shows the enlarged view of Fig. 2a with a scale bar of 2 µm and confirms the presence of spherical Cu NPs deposited on the surface of the PET fiber within a scan area of 10 µm x 10 µm. The inset of Fig. 2(b) shows the particle size distribution of Cu NPs and the average particle size lies in the range of ~500 nm.

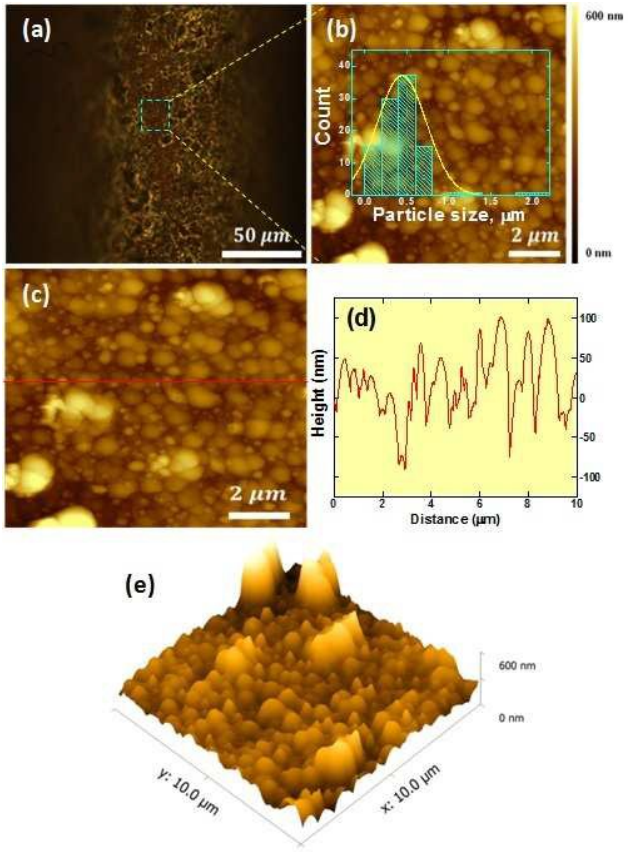

Figure 2(a-c) 2-D AFM images (d) Z-height line profile images (e) 3-D AFM image of conductive PET fiber with Cu NPs prepared at 70° C.

Furthermore, the depth profile analysis of Fig. 2(c) gives the information about the surface topography, as shown in Fig.2d. In addition, the related surface roughness R_{rms} value of Cu NPs on PET

surface is found to be 78.2 nm (±0.2). Fig. 2(e) shows the three dimensional (3D) AFM images of Cu NPs on PET fiber and the surface is almost uniform with high surface roughness value.

In order to investigate the phase purity and crystal structure of the conductive Cu fiber, X-Ray Diffraction (XRD) analysis was carried out and is shown in Fig. S1 of the ESI†. XRD pattern of Cu NPs on PET fiber deposited at 70° C displays three diffraction peak exhibited at 2θ = 43.587°, 50.555°, 74.191° which corresponds to (111), (200), and (220) planes of face-centered cubic (*fcc*) copper. The observed XRD pattern of metallic Cu is consistent with JCPDS File No. 04-836.[25] No characteristic peaks of other impurities such as copper oxide or hydroxides are identified except PET substrate peak around 2θ = 25°. Also, in order to evaluate the electrical properties of Cu NPs coated on PET fiber, current-voltage (I-V) measurement have been carried out. The I-V graph of conductive Cu NPs on PET prepared at various reaction temperatures of 50°C, 60°C and 70°C in the potential range from -0.06V to +0.06V are shown in Fig. S2 of the ESI†. It is evident from the results that the current response of conductive Cu NPs coated on PET fiber at different reaction temperature increases with respect to applied potential. Furthermore, sensing studies have been carried out for the Cu NPs on PET fiber prepared at 70° C which possess low resistivity with a high current value of 1.2 mA.

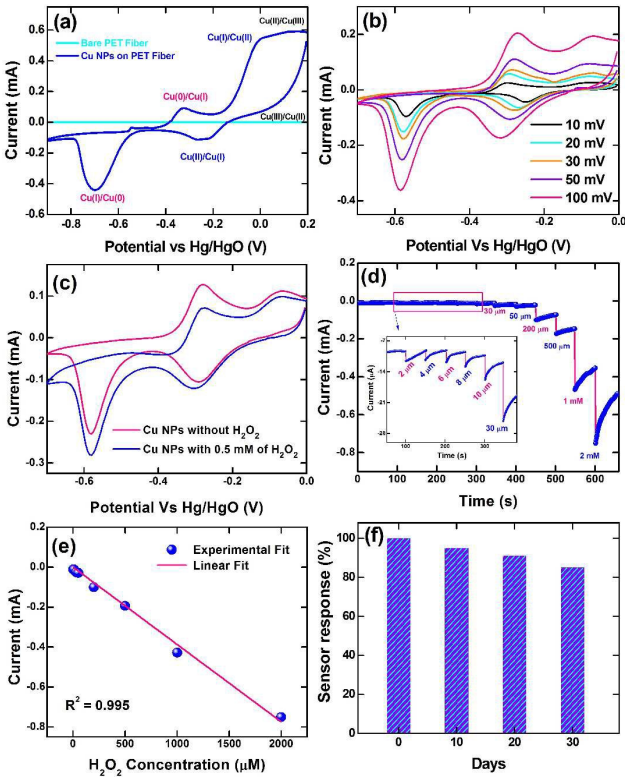

Figure 3. (a) CV curves of bare PET fiber and Cu NPs coated on PET fiber at 70° C with a scan rate of 100 mV/s (b) CV curves of Cu NPs at various scan rates (c) CV curves of Cu NPs coated PET fiber with and without H_2O_2 concentrations at a scan rate of 50 mV/s (d) Amperometric responses of the Cu NPs coated on PET fiber at pH 7 upon the successive addition of H_2O_2 in 0.1 M NaOH electrolyte. Inset: magnified image of marked rectangle region in (d). (e) Linear relationship between the current and H_2O_2 concentration (f) Stability response for Cu NPs coated PET fiber.

Fig. 3(a) shows the cyclic voltammogram (CV) of bare and Cu NPs deposited on PET fiber at 70°C in 0.1M NaOH (pH=7) with a potential range of 0 V to -0.6 V at a scan rate of 100 mV/s. No redox peaks are observed for bare non-conductive PET fiber and the current response is found to be negligible, indicating that the Cu NPs play a major role in the oxidation of H_2O_2.[26] The cyclic voltammetry of Cu NPs on PET fiber shows two obvious oxidation and reduction peaks, respectively. The anodic peaks are attributed to the formation of Cu_2O and CuO + $Cu(OH)_2$, respectively. Whereas, the cathodic peak was attributed to the reduction of CuO or $Cu(OH)_2$ to Cu_2O. Finally, Cu_2O is reduced to metallic Cu, as displayed in Fig. 3(a).[27] Hence, CV analysis confirmed that the obtained Cu NPs participates a crucial role in electrochemical performance. The CV curves of Cu NPs on PET for various scan rates are given in Fig. 3(b) which shows both anodic and cathodic peak currents are increasing linearly with increase in scan rate, indicating the surface-controlled redox phenomenon. Fig. 3(c) shows the electrochemical sensing behaviour of Cu NPs with and without H_2O_2 at a scan rate of 50 mV/s. In comparison, the CV graph of Cu NPs on PET fiber in the presence of 0.5 mM H_2O_2 exhibits an increase in peak current and this enhanced electrochemical behaviour is due to the interaction between H_2O_2 and active sites of Cu NPs.[19] Fig. 3(d) displays the amperometric response of Cu NPs deposited on PET fiber at 70° C upon the successive addition of various H_2O_2 concentrations in 0.1 M NaOH electrolyte. The inset represents the magnified image of marked rectangle region of Fig. 3(d). Furthermore, there is an increased current response upon increasing H_2O_2 concentration which exhibits the stable and efficient electrocatalytic activity of Cu NPs on PET fiber. The corresponding calibration linear curve between current and the H_2O_2 concentration is depicted in Fig. 3(e). It was observed that there is a linear increase in current with increase in H_2O_2 concentration. The sensitivity of Cu NPs on PET fiber is estimated from the slope of the calibration linear curve and it is found to be 0.387 mA μM^{-1} cm^{-2} (±0.01) with a detection limit of 2 µM and correlation co-efficient (R^2) of 0.995. The comparison of various Cu NPs based electrodes and their electrochemical sensing behaviour towards H_2O_2 is listed in Table 1.

Table 1 shows the comparison of H_2O_2 determination with various Cu NPs based modified electrodes

H_2O_2 sensor	LOD (µmol L^{-1})	Linear range (µmol L^{-1})	Applied Potential (V)	Reference
Cu/Au	2	0 - 5500	+0.6	26
Cu NPs- CuHCF/ PEDOT/GCE	0.1	1 -540	-0.20	10
CuO NF	0.005	0.05 - 0.75	-0.40	28
Cu-CuO NW	0.05	0.05 - 0.4	-0.30	29
Cu_2O-rGO	2.6	10 - 45	-0.85	30
CuO	0.8	6.0 - 2500	+0.40	31
Cu NPs	2	2.0 - 500	-0.40	**This work**

In order to identify the stability of Cu towards H_2O_2 sensing, the electrochemical analysis of the prepared Cu NPs on PET fiber was performed for duration of 30 days and their electrochemical stability is given in Fig. 3(f). There is a decrease in current response as day's increases where it retains 85% of its initial value after 30 days indicating good stability of the Cu NPs.

4. Conclusion

We have successfully fabricated conductive Cu NPs on PET fiber through electroless plating and investigated its electrochemical sensing towards H_2O_2. FESEM and AFM images confirmed the presence of spherical morphology of Cu NPs with size range of ~500 nm. XRD and EDX analysis confirmed the presence of metallic Cu NPs on the PET fiber deposited at reaction temperature of 70° C. The fabrication of Cu NPs on PET fiber exhibited a good electrochemical sensing behaviour towards H_2O_2 with an excellent sensitivity of 0.387 mA $\mu M^{-1} cm^{-2}$ and low detection limit of 2 μM. Our results showed that, the Cu NPs on PET fiber with enhanced sensitivity could be utilized as an effective electrochemical sensor towards H_2O_2.

Acknowledgements

This work was supported by the Technology Innovation Program (10041957, Design and Development of fibre-based flexible display) funded by the Ministry of Trade, industry & Energy (MI, Korea) and was also partially supported by the Student Research Fellowship program of Dongguk University.

Notes and references

[1] C. Matsubara, N. Kawamoto and K. Takamura, *Analyst*, 1992, **117**, 1781-1784.
[2] N. V. Klassen, D. Marchington and H. C. E. Mcgowan, *Anal. Chem.*, 1994, **66**, 2921–2925.
[3] P. A. Tanner and A. Y. S. Wong, *Anal. Chim. Acta*, 1998, **370**, 279–287.
[4] J. Li, P. K. Dasgupta and G. A. Tarver, *Anal. Chem.*, 2003, **75**, 1203–1210.
[5] W. Shi, X. Zhang, S. He and Y. Huang, *Chem. Commun.,* 2011, **47**, 10785–10787.
[6] B. Luo, X. Li, J. Yang, X. Li, L. Xue, X. Li, J. Gu, M. Wang and L. Jiang, *Anal. methods*, 2014, **6**, 1114-1120.
[7] Z. Liu, Y. Liu, L. Zhang, S. Poyraz, N. Lu, M. Kim, J. Smith, X. Wang, Y. Yu and X. Zhang, *Nanotechnology*, 2012, **23**, 335603-10.
[8] T. Zhang, R. Yuan, Y. Chai, W. Li and S. Ling, *Sensors*, 2008, **8**, 5141-5152.
[9] L. Zhen, Z. Lin, P. Selcuk and Z. Xinyu, *Curr. Org. Chem.*, 2013, **17**, 2256-2267.
[10] T. H. Tsai, T. W. Chen and S. M. Chen, *Int. J. Electrochem. Sci.,* 2011, **6**, 4628 – 4637.
[11] M. Liu, R. Liu and W. Chen, *Biosens. Bioelectron.,* 2013, ***45***, 206-212.
[12] M. Liu, S. He and W. Chen, *Nanoscale,* 2014, **6**, 11769-11776.
[13] S. He, B. Zhang, M. Liu and W. Chen, *RSC Adv.,* 2014, **4**, 49315-49323.
[14] J. Ju and W Chen, *Anal. Chem.,* 2015, **87**, 1903-1910.
[15] R. Z. Zhang and W. Chen, *Sci. Bull.,* 2015, **60**, 522–531.
[16] R. Zhang, S. He, C. Zhang and W. Chen, *J. Mater. Chem. B,* 2015, **3**, 4146-4154.
[17] Y. Wang, W. Wei, J. Zeng, X. Liu and X. Zeng, *Microchim. Acta,* 2008, **160**, 253- 260.
[18] A. A. Ensafi, M. Jafari-Asl, N. Dorostkar, M. Ghiaci, M. V. Martínez-Huerta and J. Fierro, *J. Mater. Chem. B,* 2014, **2**, 706-717.
[19] L. Xi, D. Shou and F. Wang, *J. Electroanal. Chem.,* 2015, **747**, 83-90.
[20] C. Jiang, A. Saha, C. Xiang, C. C. Young, J. M. Tour, M. Pasquali, and A. A. Marti, *ACS Nano,* 2013, **7**, 4503-4510.
[21] C. Jiang, A. Saha, C. C. Young, D. P. Hasim, C. E. Ramirez, P. M. Ajayan, M. Pasquali and A. A. Marti, *ACS Nano,* 2014, **8**, 9107-9112.
[22] A. Saha, C. Jiang and A. A. Marti, Carbon, 2014, **79**, 1-18.
[23] C. A. Deckert, *Plat. Surf. Finish.,* 1995, **82**, 48-55.
[24] Y. Lu, *Appl. Surf. Sci.,* 2010, **256**, 3554–3558.
[25] C. Xu, G. Liu, H. Chen, R. Zhou and Y. Liu, *J. Mater. Sci: Mater Electron.,* 2014, **25**, 2611-2617.
[26] S. Y. Tee, E. Ye, P. H. Pan, C. J. J. Lee, H. K. Hui, S. Y. Zhang, L. D. Koh, Z. Dong and M. Y. Han, *Nanoscale*, 2015, **7**, 11190-11198.
[27] V. Mani, R. Devasenathipathy, S. M. Chen, S. F. Wang, P. Devi, Y. Tai, *Electrochim. Acta,* 2015, **176**, 804–810.
[28] F. Xu, M. Deng, G. Li, S. Chen and L. Wang, *Electrochim. Acta*, 2013, **88**, 59-65.
[29] X. Zhang, G. Wang, W. Zhang, N. Hu, H. Wu and B. Fang, *J. Phys. Chem. C*, 2008, **112**, 8856-8862.
[30] A. X. Gu, G. F. Wang, X. J. Zhang and B. Fang, *Bull. Mater. Sci.,* 2010, **33**, 17-20.
[31] W. Wang, L. L. Zhang, S. F. Tong, X. Li and W. B. Song, *Biosens. Bioelectron.,* 2009, **25**, 708-14.